Molecular and Crystal Structure of a High-Temperature Polymorph of Chitosan from Electron Diffraction Data

Karim Mazeau,† William T. Winter,‡ and Henri Chanzy*,†

Centre de Recherches sur les Macromolécules Végétales, CNRS, BP 53, 38041 Grenoble Cedex 9, France, and Chemistry Department, College of Environmental Science and Forestry, State University of New York, Syracuse, New York 13210

Received June 17, 1994; Revised Manuscript Received August 19, 1994®

ABSTRACT: The crystal and molecular structure of a high-temperature polymorph of chitosan was determined by a constrained linked-atom least-squares refinement utilizing intensities derived from electron diffraction data and stereochemical restraints. In this polymorph, the chitosan chains crystallized in an orthorhombic $P2_12_12_1$ space group with cell parameters $a = 0.807$ nm, $b = 0.844$ nm, and c (chain axis) = 1.034 nm. There were two antiparallel chains per unit cell and no water of crystallization. The best projected model obtained using the base plane data coupled with stereochemical refinement gave $R = 13.3\%$. With the three-dimensional diffraction set data, the best model had R values of $R = 25.1\%$, $R'' = 17.2\%$. In this model, the chitosan molecule adopts a 2-fold helical conformation with $\Phi = -92.7°$, $\psi = -148.8°$, $\tau = 118°$, and the hydroxymethyl groups, O6, arranged in an approximately gt mode. The chitosan molecules are stabilized by two intramolecular hydrogen bonds, a strong one between O5′ and O3 and a weaker one between O5′ and O6. In addition, the crystalline structure is held together by a network of intermolecular hydrogen bonds, linking the nitrogen atoms, N2, to ring oxygen atoms, O5, of an adjacent antiparallel molecule and also to O6 of an adjacent parallel chain along the a axis.

Introduction

Chitosan, the N-deacetylated chitin, is a versatile biopolymer that is attracting much attention due to its ability to form specific complexes with a number of ions or dyes as well as a wealth of small organic molecules.[1–3] In particular, this complexation ability allows chitosan to be used commercially as an effecient agent for cleaning effluents containing hazardous transition or posttransition metal ions. It is generally accepted that the free amino group of chitosan is responsible for its complexing behavior with ions. At present, however, the precise binding mechanism and, in particular, the local molecular geometry of complexation with the amine group are still being debated. Two conflicting models are currently being considered. In the "pendant model" presented by Ogawa,[4,5] it is proposed that a single metal ion is attached as a pendant to an amino group of chitosan. In the "the bridge or chelating model" the metal ions are believed to be coordinated to several amino groups originating either from the same or from different polymer chains.[6,7]

A number of diffraction experiments have been undertaken in an attempt to elucidate the molecular geometry of chitosan either in its uncomplexed mode or when it participates in various complexes. These studies have revealed that the chitosan chain can adopt at least two different conformations in a crystalline environment, namely, a 2-fold[8–11] and an 8-fold right-handed[12,13] helical structure. In addition to these two helical conformations, a large number of crystalline polymorphs of chitosan have also been prepared and characterized.[4,10,12,15–17] These polymorphs, which differ essentially in the lateral packing of the chains, correspond either to chitosan alone or to chitosan in interaction with small molecules such as water, acids, or salts. Currently, there are only two reports[16,17] where sets of atomic coordinates for chitosan have been given. In both studies, based upon a limited number of diffraction data, chitosan is described as crystallizing in a monoclinic two-chain cell with an antiparallel packing of the molecules.

The present work, which follows earlier reports,[18,19] was undertaken to examine, in detail, the conformation and packing of chitosan crystallized in a high-temperature polymorph. The study is based on the preparation of chitosan single crystals and the recording of the intensities of their electron diffraction diagrams. In these patterns, 23 $hk0$ intensities could be measured in the crystal base plane, together with an additional 24 intensities in the upper layer lines when the crystals were rotated about their principal axes. These two data sets were used, in this report, to determine the three-dimensional crystal and molecular structure of the corresponding chitosan polymorph.

Experimental Section

Nomenclature. The recommendations and symbols proposed by the IUPAC–IUB joint commission on nomenclature are used throughout this paper.[20] A representation of the atomic labeling scheme is shown in Figure 1. The relative orientation of two contiguous residues is defined by the glycosidic bond angle τ and the torsion angles Φ and Ψ, which are defined by τ = C1′–O4–C4, Φ = O5′–C1′–O4–C4, and Ψ = C1′–O4–C4–C5. The orientation of the hydroxymethyl group is described by ω = O5–C5–C6–O6 and ω' = C4–C5–C6–O6. It is referred to as either gauche–trans (gt), gauche–gauche (gg), or trans–gauche (tg) corresponding to ω values of 60°, −60°, and 180°.[21]

Electron Microscopy and Electron Diffraction Analysis. Single crystals of chitosan were grown as described previously.[18,19] They were investigated by transmission electron microscopy under low-dose conditions. Electron diffraction patterns were recorded on Mitsubishi electron image (MEM) films, using a Philips EM 400T electron microscope equipped with a rotatable sample holder and operated at 120 kV. The $hk0$ reflections were collected from crystals aligned perpendicular to the electron beam, while $(h,k,2k)$, (h,k,k), $(h,2k,k)$, and $(h,3k,k)$ reflection classes were collected by rotation of the crystals about a^* by ±57°, ±38°, ±22°, and ±15°

* Corresponding author.
† Centre de Recherches sur les Macromolécules Végétales, affiliated with the University Joseph Fourier of Grenoble, France.
‡ State University of New York.
® Abstract published in *Advance ACS Abstracts,* November 1, 1994.

0024-9297/94/2227-7606$04.50/0

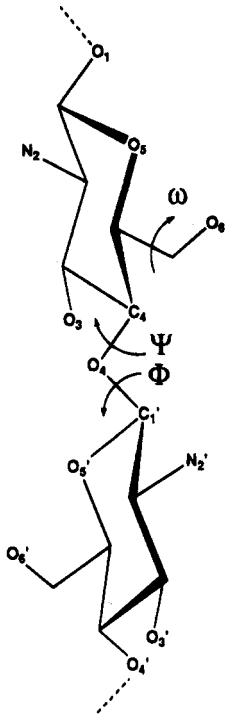

Figure 1. Atomic labeling for the chitosan chain, and designation of the torsion angles Φ, Ψ, and ω.

corresponding to the [0,2,-1], [0,-1,1], [0,-1,2], and [0,-1,3] zones, respectively. Similarly, rotation of the crystals about b^* by ±57°, ±38°, and ±17° allowed the collection of the (*h*,*k*,2*h*), (*h*,*k*,*h*) and (3*h*,*k*,*h*) reflection classes corresponding to the [-2,0,1], [-1,0,1] and [-1,0,3] zones.

The intensities of *hk*0 and *hkl* reflections were measured by scanning the diffractograms with a Joyce-Loebl recording microdensitometer. The intensity of each reflection was taken as the height of the peak in the tracing, corrected for the background density. The intensities were corrected to account for the film linearity by using a polynomial fit of the characteristic curve of the MEM films, where the optical density was measured as a function of the electron dose. All the *hk*0 diffractograms were scaled with respect to one another by summing all the observed intensities in each diagram and scaling these sums. After scaling, the intensity of each reflection taken from the series of diagrams was averaged and individual $F(hk0)$ were taken as the square root of the corresponding intensity. In the *hkl* diagrams, those spots with *hk*0 indices were employed as standards to scale these patterns with respect to the *hk*0 diffractograms. $F(hkl)$ were taken as the square root of the corresponding intensity. In this work, no attempt was made to account for a dynamic effect, which was believed to be small since the crystalline lamellae were only of the order of 10 nm thick, and in addition, the crystal consisted only of atoms of low atomic number. Occasional thick crystals gave diagrams with forbidden reflections such as 100 or 010. These reflections, which were always weak, were not accounted for.

The *hk*0 data set has a resolution of 0.15 nm. It consisted of 17 measurable independent reflections, 6 systematic absences for odd orders of *h*00 and 0*k*0, and 6 other reflections below the observational threshold. The *hkl* data set contained 18 observable reflections together with 6 below the observational threshold. Within each diagram, the unobserved reflections within the sphere of diffraction were assigned relative intensities of one-third of the minimum observable value in the corresponding diffractogram.

For the weighted refinement of the structure, a weight of 1 was given to the $F(hk0)$. A weight of 0.75 was selected for the $F(hkl)$ with $l \neq 0$ if the intensity of the corresponding spot did not differ from one diagram to the next by more than 25%. A weight of 0.50 was given to the other observed $F(hkl)$ with $l \neq 0$ if the intensity of the corresponding spot differed from one to the next by more than 25%.

Modeling. The starting coordinates of glucosamine, the monomer of chitosan, were first deduced from the Arnott and Scott "standard sugar ring" geometry.[22] A version of the linked-atom least-squares (LALS) refinement program[23] modified for the use of electron diffraction data[24] was used throughout the refinement of the structure. The form factors for electron diffraction for atomic species C, O, N, and H were taken from the International Tables of X-ray Crystallography. Contact parameters used in the stereochemical refinement are those of Arnott and Winter.[25] Calculations were performed either on an IBM 3090 computer at Syracuse or on a Sun workstation at the CERMAV. Molecular drawings were produced on an IRIS Silicon Graphics workstation with the the QUANTA software.[26]

Results

Figure 2 is a transmission electron micrograph of a crystal of chitosan together with its *hk*0 electron diffractogram diagram. Similar patterns were recorded for crystals rotated about a^* and b^*. These patterns, which were identical to those published earlier,[18] are not reproduced here. As also determined earlier for such crystals, the polymer is crystallized in the $P2_12_12_1$ space group and with unit cell dimensions $a = 0.807$ nm, $b = 0.844$ nm, and c (chain axis) = 1.034 nm. This cell contains two antiparallel chitosan chains, each molecule being located on a 2-fold screw axis parallel to c, and there are no water molecules within the unit cell.

The chitosan chain was built and its energy was further minimized with the LALS program after setting the chain along a 2-fold screw axis and constraining it to a helical repeat of 1.034 nm. Depending upon the orientation of the primary hydroxymethyl groups, three different models, namely, gg, gt and tg, were then generated with initial torsion angle ω values of −60°, +60°, and 180°, respectively.

For each model, a chitosan chain was positioned within the unit cell, aligning the chain helix axis parallel to c and coincident with a crystallographic 2_1 axis. The other chain of the crystal were then generated by the $P2_12_12_1$ symmetry. For each of the three model, refinement of the structure was initiated by rotating an independent chitosan chain about its helix axis in 10° increments and subsequent generation of its symmetry-related chain within the unit cell. This rotation was defined by the value of a variable parameter, μ, the cylindrical polar coordinate angle between a vector parallel to the a edge of the unit cell and a vector linking the helix origin to the glycosidic oxygen, O4, chosen as the root atom of chitosan. The nonbonded energy of interaction E[27] and the crystallographic residual R[28] from the *hk*0 diffraction data were computed as a function of μ for the three models (Figure 3). In each case, values of μ smaller than 90° led to R factors that were very large, while there were two local minima between 90° and 180° where both the energy and the R factor were minimal. One was located between 120° and 130° and the other near 160°. These two values of μ were then used for further refinement of the three models. This optimization showed that refinements which started from an orientation angle near 120° led to lower final reliability factors than those starting from $\mu = 160°$. For this reason, only the μ angle near 120° was considered. Table 1 shows that, among the three models, the one with the gt conformation was superior with a R factor of 13.3% as opposed to $R = 19.2\%$ for the gg and $R = 16.1\%$ for tg. The optimized gt model had a μ value of 123.41° and an energy of 4.69 units.

Each of these three models, optimized as in Table 1, were further refined using the three-dimensional dif-

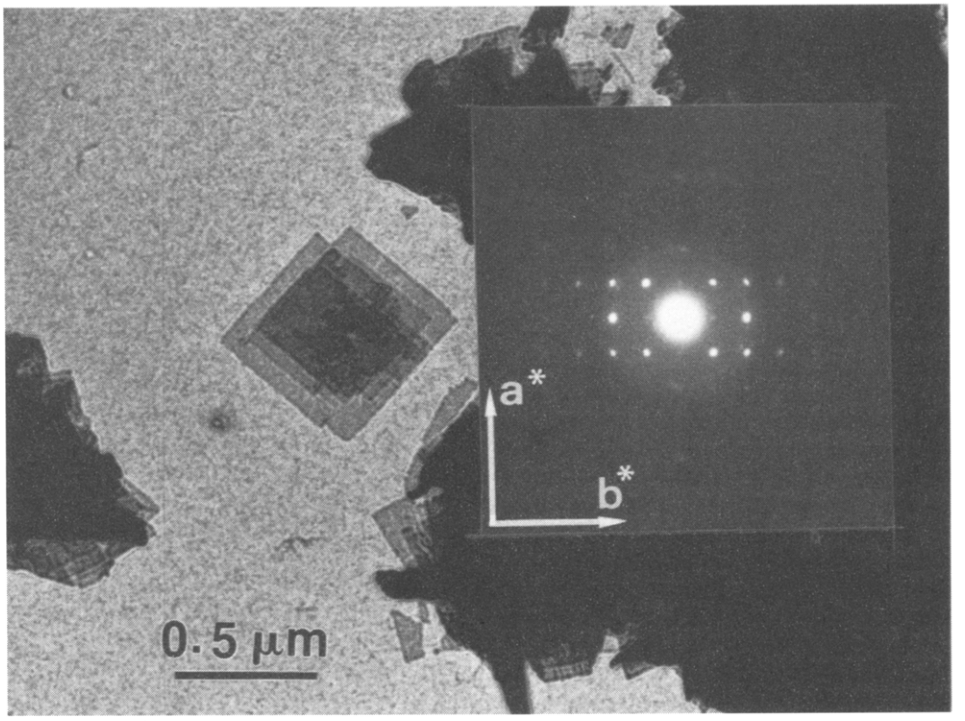

Figure 2. Typical transmission electron micrograph of a chitosan single crystal and its electron diffraction diagram (inset).

Table 1. Final Crystallographic Residual R_{hk0}, Nonbonded Energy of Interaction E (in Arbitrary Units), and Chain Orientation Angle μ for the Three Models with Different Hydroxymethyl Conformation

	gg	gt	tg
R_{hk0} (%)	19.22	13.33	16.10
E	4.89	4.69	5.00
μ (deg)	123.40	123.41	122.31

[a] Projected on the *ab* plane of chitosan.

Table 2. Final Crystallographic Residual R_{hkl} and R''_{hkl}, Nonbonded Energy of Interaction E (in Arbitrary Units), and Chain Translation W Along the c Axis for the Three Models with Different Hydroxymethyl Conformations

	gg	gt	tg
R_{hkl} (%)	26.39	25.10	27.96
R''_{hkl} (%)	19.47	17.19	20.45
E	5.17	4.21	5.14
W	0.1838	0.1835	0.1835

fraction data by systematically translating the helices parallel to the c axis in steps of $c/20$ (variable W, Figure 4). This was followed by a full refinement where all the conformational and packing parameters were optimized. For each model, there was only one position close to $W = 0.2$ where the R factor as well as the energy exhibited a minimum (Table 2). Based on energy criteria, the absence of any bad contact, and the best R factor, the *gt* model is again selected as the best. It has an R of 25.1%, and R'' of 17.2%, and a packing energy of 4.21 units. Its difference with the *gg* model, the second best, is however not as large as in the case of the refinement of the *hk*0 projection.

Final values of the varied parameters of the final best model for the high-temperature orthorhombic chitosan polymorph are given in Table 3, while details of its hydrogen-bonding pattern are summarized in Table 4 and its atomic coordinates are given in Table 5. The comparisons of calculated and observed structure factor amplitudes are given in Table 6, showing generally good agreement. In Figure 5, the chitosan crystal structure is shown in an *ab* projection. The *ac* and *bc* projections

Table 3. Summary of Varied Parameters and Their Final Values

parameter	final value	parameter	final value
Φ (deg)	−92.65	τ (deg)	118.0
Ψ (deg	−148.79	μ (deg)	123.41
ω (deg)	47.68	W	0.1835

Table 4. Summary of Hydrogen Bond Interactions Stabilizing the Structure of Chitosan

donor atom	acceptor atom	d (nm)	angle (deg)	symmetry[a]
O3	O5′	0.26	102.0 (C3−O3···O5′)	I···I
O6′	O3	0.32	107.7 (C6′−O6′···O3)	I···I
N2	O5	0.35	93.1 (C2−N2···O5)	I···II
N2	O6	0.26	131.4 (C2−N2···O6)	I···III

[a] I···II and I···III, intermolecular interactions. The unit II is generated by $(x', y', z') = (a/2 + x, -b/2 - y, -z)$; the unit III is generated by $(x', y', z') = (a + x, y, z)$.

are presented in Figure 6 while Figure 7 illustrates details of the inter- and intramolecular hydrogen bonds which hold the structure together.

Discussion

The structure of chitosan described in this study is based on a monomer geometry derived from that of the average pyranose residue given by Scott and Arnott.[22] Other attempts (not presented here) were also made to define the starting monomer geometry by using the MM2CARB molecular mechanics program.[29] This approach, however, was not successful as it invariably led to chitosan conformations with glycosidic bond angles of the order of 120°, out of the range expected for such a polymer.[22] In the present case, the bond lengths, bond angles, and torsion angles (data not shown) that were calculated for the monomer residue are in good agreement with the corresponding parameters recorded in the crystal structures of α-D-glucosamine.[30-32]

In terms of helical repeat, our study shows that the chitosan molecules are organized as regular 2-fold helices with the torsion angles Φ and Ψ having the

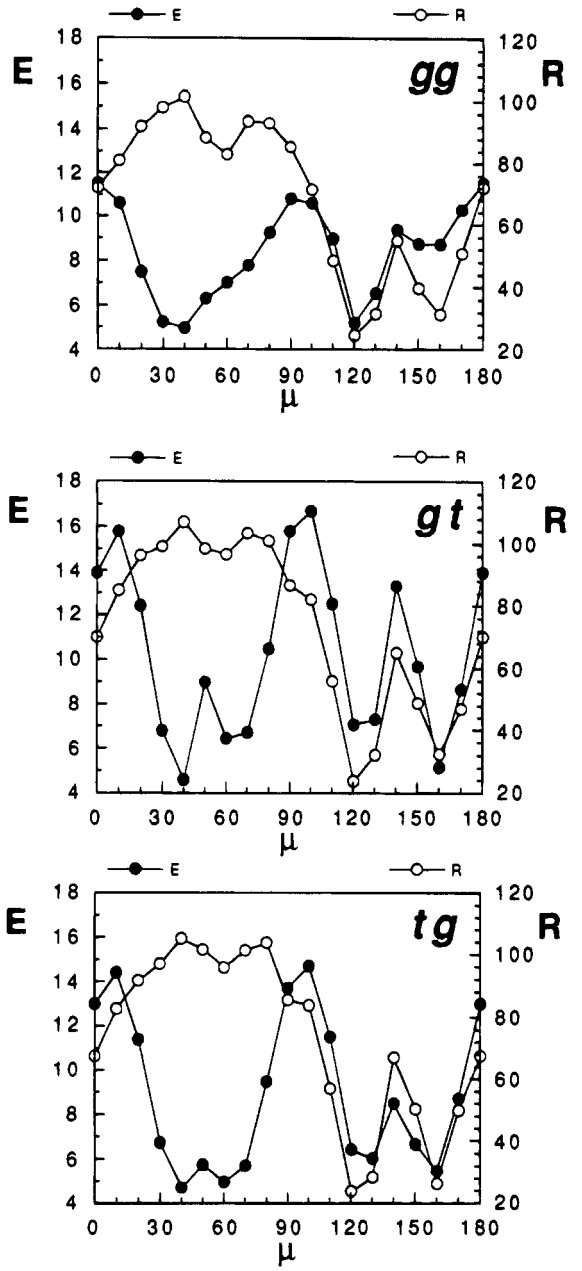

Figure 3. Reliability factor R_{hk0} and nonbonded energy of interaction E as a function of the orientation angle μ for the three conformations of the hydroxymethyl group: tg gg, and gt.

values of −92.65° and −148.79°, respectively, while the glycosidic bond angle τ took the value of 118°. These values correlate well with Φ and Ψ of −79.5° and −165.9° that are measured in the crystal structure of *N,N'*-diacetylchitobiose[33] or −83.2° and −168.3° that are computed for chitobiose in the isolated state after energy minimization.[34] In fact, this optimized conformation of chitobiose exhibits considerable similarity to that of the present polymer. In both cases, the molecules are stabilized by two intramolecular hydrogen bonds and in both cases, the *gt* conformation is found for the orientation of O6. In our chitosan, the atom O3 is involved with two intramolecular hydrogen bonds: a strong one between O5′ and O3 and a weaker one between O6′ and O3 (Table 4). As for the conformation at O6 (Table 3), its ω value is refined to 47.68°, a value quite close to the canonical *gt* conformation where ω takes the value of 60°. The *gt* conformation of the hydroxymethyl group of chitosan is supported by ^{13}C CP/MAS data on our crystals, which showed that the

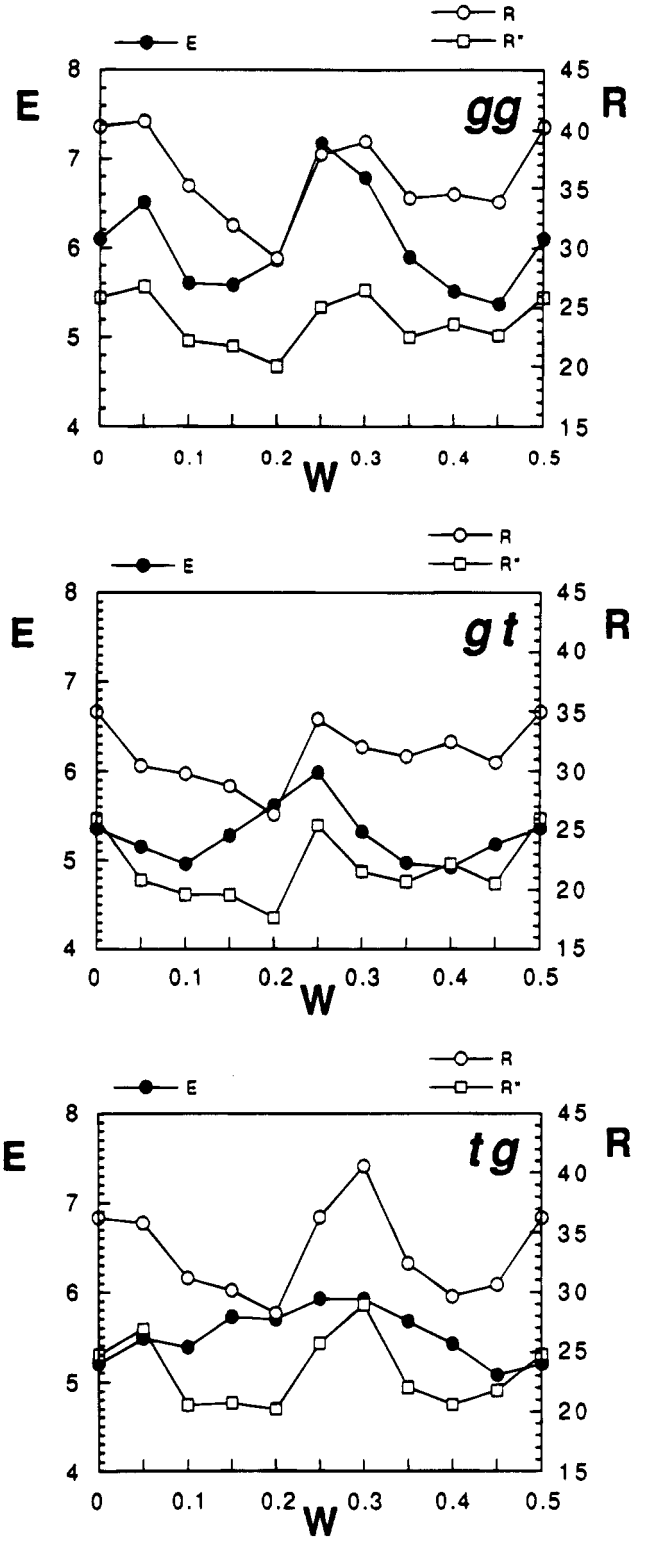

Figure 4. Reliability factors R_{hkl} and R''_{hkl} together with nonbonded energy of interaction E as a function of the translation W for the three conformations of the hydroxymethyl group: tg, gg, and gt.

resonance at C6 occurred as a singlet at 62.6 ppm.[19] This value is in the range of 62.5−64.5 ppm which, according to the scale proposed by Horii *et al.*,[35] corresponds to the *gt* conformation in the glucose series.

As described in Figures 5−7, the chitosan chains are held together by a tight network of intermolecular hydrogen bonds. This network is essentially organized around the nitrogen, which acts as a donor for the O6 of an adjacent molecule and O5 of another. The distance between the nitrogen and O6 is however much shorter

Table 5. Fractional Atomic Coordinates of Chitosan

atom	x	y	z
C1	0.242 06	−0.000 93	0.586 20
C2	0.330 09	−0.073 67	0.485 43
C3	0.316 56	−0.010 86	0.347 57
C4	0.170 12	−0.003 37	0.307 16
C5	0.088 62	0.064 65	0.416 64
C6	−0.059 83	0.064 96	0.387 40
O1	0.247 61	−0.069 53	0.706 79
O3	0.389 13	−0.088 75	0.252 09
O4	0.155 88	0.069 53	0.189 79
O5	0.106 53	−0.004 11	0.541 43
O6	−0.148 68	0.103 38	0.492 25
N2	0.471 59	−0.071 02	0.529 39
H1	0.272 93	0.098 82	0.597 28
H2	0.299 89	−0.174 00	0.478 51
H3	0.355 94	0.086 46	0.349 38
H4	0.133 20	−0.100 34	0.291 06
H5	0.119 98	0.164 33	0.426 88
H61	−0.079 94	0.131 66	0.308 84
H62	−0.090 33	−0.031 67	0.359 88
HNa	0.504 18	−0.108 28	0.621 99
HNb	0.526 78	−0.098 45	0.444 38

Table 6. Final Values of the Observed $F_o(hkl)$ and Calculated $F_c(hkl)$ Structure Amplitudes

h	k	l	$F_c(hkl)$	$F_o(hkl)$
0	2	0	50.44	50.56
0	4	0	4.65	5.60
1	1	0	31.35	33.88
1	2	0	32.92	32.72
1	3	0	18.94	20.75
1	4	0	12.50	13.02
1	5	0	7.59	10.05
2	0	0	2.81	6.18
2	1	0	1.68	4.51
2	2	0	4.51	6.44
2	3	0	1.07	5.03
2	4	0	6.71	5.92
2	5	0	4.46	4.25
3	1	0	0.35	2.44
3	2	0	6.31	4.38
3	3	0	1.06	2.44
3	4	0	0.92	2.44
4	0	0	14.13	17.26
4	1	0	0.75	2.44
4	2	0	5.69	4.82
4	3	0	0.21	2.44
5	1	0	2.78	4.25
5	2	0	1.61	2.44
0	1	2	17.82	18.11
1	1	2	8.96	3.89
2	1	2	9.16	8.02
1	1	1	2.83	3.43
2	1	1	4.05	3.57
3	1	1	3.87	3.31
0	3	3	3.67	3.57
1	2	1	4.81	3.14
2	2	1	4.91	5.62
3	2	1	6.08	4.30
2	0	1	5.40	5.02
3	0	1	16.07	9.77
1	3	1	1.94	2.38
1	4	1	1.19	2.25
3	1	2	4.57	2.66
0	2	2	3.92	3.39
2	2	2	2.53	3.22
3	2	2	7.92	3.22
0	2	4	1.51	1.54
1	2	2	6.58	1.86
0	2	1	5.88	1.82
2	0	2	1.95	1.30
2	3	2	5.51	1.30
1	3	2	7.44	2.24

than that with O5: 0.26 nm versus 0.35 nm. Another interesting feature of our chitosan structure is that it appears devoid of any crystallization water, despite the

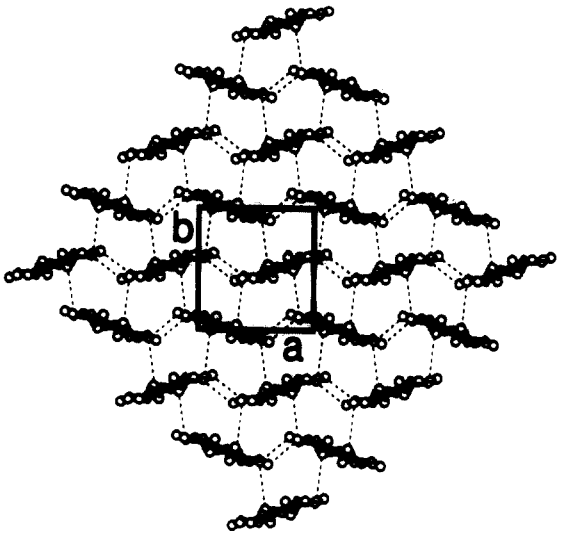

Figure 5. Structure of the chitosan viewed as a projection of the unit cell into the *ab* plane and outlining the shape of the crystals with their {110} growth planes. In this projection each chitosan molecule is viewed with its chain axis vertical. The dotted lines correspond to the hydrogen bonds.

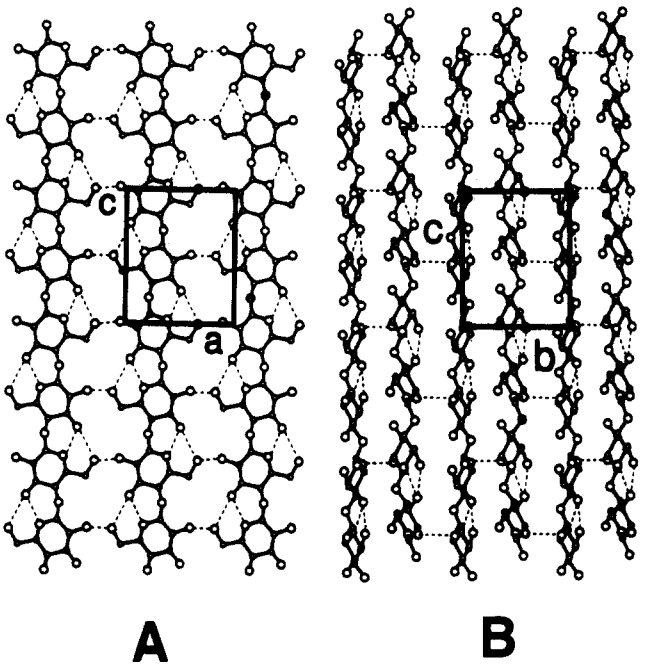

Figure 6. Structure of the chitosan viewed as a projection of the unit cell into the *ac* plane (A) and *bc* plane (B). The dotted lines correspond to the hydrogen bonds.

fact that the crystals were grown in an aqueous environment. This is likely due to the high temperature at which the crystals were grown.[18] In similar cases with dextran or mannan, it was also observed that the crystals of these polysaccharides grew as anhydrous polymorphs when temperatures higher than 100 °C were selected.[36,37] On the other hand, when crystallization temperatures lower than 90 °C were chosen, the resulting low-temperature crystalline polymorphs contained water within their crystalline lattices.[37,38] In the present case, the high-temperature polymorph of chitosan behaves as the corresponding polymorphs of dextran and mannan and is indeed anhydrous. Our attempts to grow chitosan crystals at temperatures lower than 100 °C in order to obtain the elusive crystals of a chitosan hydrate have been so far unsuccessful.

The chitosan structure presented in this study differs somewhat from the three chitosan structures whose

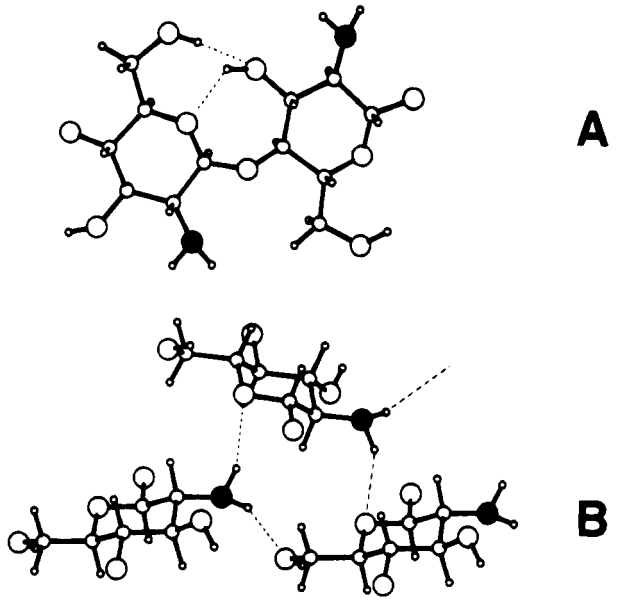

Figure 7. Detail of the hydrogen-bonding system: (A) environment of the O3 and its intramolecular hydrogen bonds; (B) environment of the nitrogen atom of chitosan and its intermolecular hydrogen-bonding pattern. In both (A) and (B), the nitrogen atoms are shown in black.

coordinates have been reported by Sakurai *et al.*[16,17] The structures described by these authors are monoclinic, and each of them contains one molecule of water per residue. However, as in our study, their models consist of two antiparallel chains and one of their structures, the so-called L-2 structure, presents a packing arrangement that resembles the one shown in Figures 5 and 6. The discrepancy between Sakurai structures and ours may be because his crystalline samples were not prepared in the same way as ours. His specimens consisted of films that were cast at room temperature from formic acid solutions. His best crystalline film, namely, the L-2 sample, was further washed with aqueous NaOH and during this treatment it is likely that water was allowed to penetrate within the crystalline lattice. Another possibility for the discrepancy between our structure and those of Sakurai *et al.*[16,17] may have its origin in the precision and number of diffraction data used for the crystal refinement. Indeed, L-2, the best structure of Sakurai *et al.*[16,17] is based on 10 independent diffraction data out of which 2 are composites with contributions from more than one diffracting plane. In his monoclinic mode, two independent glucosamine moieties, i.e., 22 non-hydrogen atoms, plus some water have to be determined from these 10 diffraction data. Our structure appears more reliable as it was deduced from a set of 47 diffraction intensities and there is only one independent sugar residue, i.e., 11 non-hydrogen atoms, to position within the unit cell.

In terms of unit cell dimensions, the present chitosan structure bears a strong similarity to the high-temperature polymorph reported by Ogawa *et al.*,[11] except that our *b* parameter is half of that of these authors. Their long *b* parameter is based on the occurrence of two very weak reflections indexed as 130 (0.462 nm) and 013 (0.340 nm) in their system. As none of our base plane pattern showed a reflection at 0.462 nm, or any other position requiring a doubling of the *b* axis, we are quite confident about our unit cell with a short *b* parameter. In the case of Ogawa *et al.*, their stretched films were first cast from aqueous solution at room temperature and then further annealed at high temperature in an aqueous environment. Their crystallization treatment differs from our approach, where the crystals were grown directly from solution at high temperature. Thus, it may be that we have the same polymorph as they do, but, in their case, a small fraction of a hydrated chitosan polymorph, e.g., the "hydrated tendon chitosan", remained even after annealing at high temperature. Then the major component of their high-temperature polymorph would be exactly the same as the form whose structure we present in this report.

If one excludes the crystalline complexes of chitosan and the high-temperature polymorph of Ogawa *et al.*[11]—that we believe is identical to our structure—there remain at least six other crystalline polymorphs of chitosan that have been reported. The chitosan crystals reported here differ markedly from most of the other crystalline polymorphs listed for this biopolymer. Our unit cell and conformation are totally different from those given by Cairns *et al.*[13] and this indicates at least two distinct families of chitosan structures. Although out unit cell has the same *c* parameter as those reported by Clark and Smith,[8] Samuels,[9] and Sakurai *et al.*,[16,17] our *a* and *b* parameters are quite different from those given by these authors. In addition, our space group is orthorhombic as are those of Clark and Smith or Samuels, but differs from the monoclinic systems proposed by Sakurai *et al.*[16,17] This diversity in cell parameters of chitosan may reflect the unusual conformational and packing versatility of this biopolymer. It may also be that several of the polymorphs that have been reported may, in fact, be mixtures of two or more crystalline allomorphs of chitosan. This possibility has been suggested by Ogawa *et al.*[14] who indicated that one of the polymorphs reported by Sakurai *et al.*,[16,17] the so-called 1−2, was actually a mixture of hydrated and anhydrous crystals. At this stage, we feel that the polymorphism of chitosan is far from being fully understood and that one should try to prepare batches of well-characterized single crystals of the other allomorphs. The chitosan hydrate, sometimes called "tendon chitosan" would be the most interesting candidate as it is particularly amenable to solid-state conversion through a series of salts.[12] Modeling such transformations with single crystals should help to elucidate the critical geometric factors that control the complexing behavior of chitosan.

The preparation of single crystals of well-characterized and totally deacetylated chitosan is limited to fractions of low molecular weight material having a DP of 35. Thus, although our crystals consist of an antiparallel array of chitosan chains, they do not result from a regular chain-folding mechanism as the thickness of the crystalline lamellae are roughly equivalent to the fully stretched chains of DP 35. When samples of higher molecular weights were used, a shapeless polycrystalline precipitate was obtained. Therefore, it seems that a regular chain folding is unlikely for chitosan, which thus resembles other β-(1→4)-linked polysaccharides such as chitin,[39] cellulose,[40] mannan,[41] etc. Indeed, these polysaccharides are amenable to the formation of lamellar single crystals only with a low molecular weight polymer fraction, where the crystals result only from the crystallization of short polymer stems.

A final interesting aspect of this work is the preparation of polymer single crystals and the use of electron diffraction data sets derived from such crystals as the sole source of structure amplitudes for the eventual solution of their three-dimensional structure. The

single crystals, such as those of chitosan described here, appear to yield a reliable *hk*0 diffraction data set. Indeed, this set, consisting of 23 independent diffraction data, leads to a projected chitosan structure devoid of any short contact and whose reliability factor R is 13.3%. The situation is less favorable with the use of the *hkl* diffraction data as the best structure still has crystallographic residuals R and R'' of 25.1% and 17.2%. We feel that these values could be substantially reduced if the technique of recording the *hkl* diagrams could be improved by taking the patterns on parts of the specimens that have not been irradiated previously. In our laboratory, the recording of an *hkl* diagram requires first the identification of the crystallographic axes on an image intensifier connected to the electron microscope. This is followed by the rotation of the crystal to bring one of these axes into coincidence with the tilt axis of the stage. Even under reduced beam intensity, these operations are carried out in the electron beam, which therefore may induce some beam damage to the crystals. Thus, the diffraction intensities that are measured may not correspond to the initial sample but rather to crystals that have been substantially damaged and, in particular, cross-linked. Use of the evolving new computer-controlled goniometric stages should allow minimization of these artifacts since they would permit the alignment of a given crystal in a series of specific orientations, in total darkness, once the orientation of the matrix of the crystal axes relative to the instrumental axes is known.

Acknowledgment. The authors are indebted to N. Cartier for the gifts of chitosan crystals that were used throughout this work. They thank also J. Sugiyama for his help in measuring and correcting the diffraction intensities.

References and Notes

(1) Muzzarelli, R. A. A. *Chitin*; Pergamon Press: New York, 1973.
(2) Muzzarelli, R. A. A. *Natural Chelating Polymer*; Pergamon Press: Oxford, UK, 1973.
(3) Roberts, G. A. F. *Chitin Chemistry*; MacMillan: London 1992
(4) Ogawa, K.; Oka, K.; Miyanishi, T.; Hirano, S. In *Chitin, Chitosan and Related Enzymes*; Zikakis, J. P., Ed.; Academic Press: Orlando, FL, 1984; pp 327–345.
(5) Ogawa, K. *Nippon Nogeikagaku Kaishi* **1988**, *62*, 1225.
(6) Yaku, F.; Muraki, E.; Tsuchiya, K.; Shibata, Y.; Koshijima, T. *Cellulose Chem. Technol.* **1977**, *11*, 421.
(7) Schlick, S. *Macromolecules* **1986**, *19*, 192.
(8) Clark, G. L.; Smith, A. F. *J. Chem. Phys.* **1937**, *40*, 863.
(9) Samuels, R. J. *J. Polym. Sci., Polym. Phys. Ed.* **1981**, *19*, 1081.
(10) Sakurai, M.; Takagi, M.; Takahashi, T. *Sen-i Gakkaishi* **1984**, *40*, T246.
(11) Ogawa, K.; Hirano, S.; Miyanishi, T.; Yui, T.; Watanabe, T. *Macromolecules* **1985**, *17*, 973.
(12) Ogawa, K.; Inukai, S. *Carbohydr. Res.* **1987**, *160*, 425.
(13) Cairns, P.; Miles, M. J.; Morris, V. J.; Ridout, M. J.; Brownsey, G. J.; Winter, W. T. *Carbohydr. Res.* **1992**, *235*, 23.
(14) Ogawa, K.; Yui, T.; Miya, M. *Biosci. Biotechnol. Biochem.* **1992**, *56*, 858.
(15) Ogawa, K. *Agric. Biol. Chem.* **1991**, *55*, 2375.
(16) Sakurai, K.; Shibano, T.; Kimura, K.; Takahashi, T. *Sen-i Gakkaishi* **1985**, *41*, T-361.
(17) Sakurai, K.; Shibano, T.; Takahashi, T. *Mem. Fac. Eng., Fukui Univ.* **1985**, *33*, 71.
(18) Cartier, N.; Domard, A.; Chanzy, H. *Int. J. Biol. Macromol.* **1990**, *12*, 289.
(19) Cartier, N.; Mazeau, K.; Domard, A.; Chanzy, H. In *Advances in Chitin and Chitosan*; Brine, C. J., Sandford, P. A., Zikakis, J. P., Eds.; Elsevier Applied Science: London and New York, 1992; pp 155–164.
(20) IUPAC–IUB Joint Commission on Biochemical Nomenclature. *Eur. J. Biochem.* **1983**, *131*, 5.
(21) Marchessault, R. H.; Pérez S. *Biopolymers* **1979**, *18*, 2369.
(22) Arnott, S.; Scott, W. E. *J. Chem. Soc., Perkin Trans. 2* **1972**, 324.
(23) Smith, P. J. C.; Arnott, S. *Acta Crystallogr.* **1978**, *A34*, 3.
(24) Chanzy, H.; Pérez, S.; Miller, D.; Paradossi, G.; Winter, W. T. *Macromolecules* **1987**, *20*, 2407.
(25) Arnott, S.; Winter, W. T. *Fed. Proc., Fed. Am. Soc. Exp. Biol.* **1977**, *36*, 73.
(26) Quanta 33, Molecular Simulations, Burlington, MA.
(27) The nonbonded energy of interaction is defined as in refs 23 and 25. It is applied to all pairwise interactions between atoms i and j when the distances between them is less than a "standard" value.
(28) The crystallographic residuals R and R'' are calculated as follows: $R = \sum(kF_0 - F_c)^2/\sum k^2F_o^2$; $R'' = \sum[w(k^2F_o^2 - F_c^2)]/\sum wk^2F_o^2$, where k is the scale factor.
(29) Tvaroska, I.; Pérez, S. *Carbohydr. Res.* **1986**, *149*, 389.
(30) Chu, S. S. C.; Jeffrey, G. A. *Proc. R. Soc.* **1965**, *285*, 470.
(31) Chandrasekharan, R.; Mallikarjunan, M. *Z. Kristallogr.* **1969**, *129*, 29.
(32) Ramachandran, G. N.; Chandrasekharan, R.; Chandrasekharan, K. S. *Biochim. Biophys. Acta* **1967**, *148*, 317.
(33) Mo, F.; Jensen, L. H. *Acta Crystallogr.* **1978**, *B34*, 1562.
(34) Yui, T.; Kobayashi, M.; Kitamura, S.; Imada, K. *Biopolymers* **1994**, *34*, 203.
(35) Horii, F.; Hirai, A.; Kitamaru, R. *Polym. Bull.* **1983**, *10*, 357.
(36) Chanzy, H.; Excoffier, G.; Guizard, C. *Carbohydr. Polym.* **1981**, *1*, 67.
(37) Chanzy, H.; Grosrenaud, A.; Vuong, R.; Mackie, W. *Planta* **1984**, *161*, 320.
(38) Guizard, C.; Chanzy, H.; Sarko, A. *J. Mol. Biol.* **1985**, *183*, 397.
(39) Persson, J. E.; Domard, A.; Chanzy, H. *Int. J. Biol. Macromol.* **1992**, *14*, 221.
(40) Buléon, A.; Chanzy, H.; Froment, P. *J. Polym. Sci., Polym. Phys. Ed.* **1982**, *20*, 1081.
(41) Chanzy, H.; Dubè, M.; Marchessault, R. H.; Revol, J. F. *Biopolymers* **1970**, *18*, 887.